Earth and Planetary Science Letters 475 (2017) 152–159

Contents lists available at ScienceDirect

Earth and Planetary Science Letters

www.elsevier.com/locate/epsl

Influence of pore pressure change on coseismic volumetric strain

Chi-Yuen Wang [a,*], Andrew J. Barbour [b]

[a] Dept. Earth and Planetary Science, University of California, Berkeley, CA 94720, United States
[b] Earthquake Science Center, U.S. Geological Survey, Menlo Park, CA 94025, United States

ARTICLE INFO

Article history:
Received 2 June 2017
Received in revised form 20 July 2017
Accepted 21 July 2017
Available online xxxx
Editor: P. Shearer

Keywords:
coseismic strain
dislocation model
pore pressure

ABSTRACT

Coseismic strain is fundamentally important for understanding crustal response to changes of stress after earthquakes. The elastic dislocation model has been widely applied to interpreting observed shear deformation caused by earthquakes. The application of the same theory to interpreting volumetric strain, however, has met with difficulty, especially in the far field of earthquakes. Predicted volumetric strain with dislocation model often differs substantially, and sometimes of opposite signs, from observed coseismic volumetric strains. The disagreement suggests that some processes unaccounted for by the dislocation model may occur during earthquakes. Several hypotheses have been suggested, but none have been tested quantitatively. In this paper we first examine published data to highlight the difference between the measured and calculated static coseismic volumetric strains; we then use these data to provide quantitative test of the model that the disagreement may be explained by the change of pore pressure in the shallow crust. The test allows us to conclude that coseismic change of pore pressure may be an important mechanism for coseismic crustal strain and, in the far field, may even be the dominant mechanism. Thus in the interpretation of observed coseismic crustal strain, one needs to account not only for the elastic strain due to fault rupture but also for the strain due to coseismic change of pore pressure.

1. Introduction

Coseismic deformation of Earth's crust is fundamentally important for understanding how Earth's crust responds to transient stress changes. Various measurements, from long-baseline geodesy to well-bore strain, have been used to document such deformation. Press (1965) first used elastic dislocation theory to interpret observed coseismic deformation on strainmeters. Since then the dislocation model has been extensively used in interpreting coseismic deformation in terms of shear displacements on ruptured faults. This procedure has been widely adopted by seismologists and geodesists to invert InSAR and GPS ground displacement data to resolve slip distribution on ruptured faults (e.g., Okada, 1985; Burgmann et al., 1997; Bletery et al., 2016) and to predict coseismic stress changes and triggered seismicity (e.g., Rybicki, 1973; Stein and Lisowski, 1983; Harris and Simpson, 1992; Simpson and Reasenberg, 1994; King et al., 1994; Hughes et al., 2010).

The dislocation model has also been applied to the interpretation of earthquake-produced volumetric deformation, especially in the interpretation of coseismic change of groundwater level or pore pressure (e.g., Quilty and Roeloffs, 1997; Johnston et al., 2006; Kroll et al., 2017). Although some studies showed agreement between the predicted volumetric strain and the observed change in the near field of moderate and large earthquakes, most studies showed that the predicted volumetric strains from dislocation model are either much smaller than, or of opposite sign from, the observed strain both in the near and in the far fields of earthquakes (e.g., Roeloffs, 1998; King et al., 1994; Qiu and Shi, 2003, 2004; Koizumi et al., 2004; Fu et al., 2011; Roeloffs et al., 2015; Barbour et al., 2015; Zhang et al., 2017).

Several hypotheses have been proposed to explain the discrepancies between the observed coseismic volumetric strain and that predicted from the theoretical dislocation model. Quantitative testing of these hypotheses, however, is difficult and not available. The most commonly suggested cause of the discrepancies is local heterogeneities near the site of strain measurement, either local geologic and/or topographic heterogeneities (e.g., Beaumont and Berger, 1975) or local deformation triggered by dynamic strains (Roeloffs, 2010; Barbour et al., 2015). Quilty and Roeloffs (1997) suspected that the discrepancies might be due to different characteristics of wells. Qiu and Shi (2003) proposed that uncertainties in the source parameters of the dislocation model might be the cause; they also mentioned factors such as changes in the mechanical properties of faults and wall rocks, pore pressure and ground-

* Corresponding author.
E-mail address: chiyuen@berkeley.edu (C.-Y. Wang).

http://dx.doi.org/10.1016/j.epsl.2017.07.034
0012-821X/

water flow, but offered little details. Fu et al. (2011) suggested that the discrepancies might have been caused by local crustal structure and initial stress. Roeloffs et al. (2015) suggested that ground motion may be the controlling mechanism. Zhang et al. (2017) suggested that coseismic changes of groundwater level may be the cause for coseismic change of volumetric strain.

Here we first compile published results and compare the observed coseismic volumetric strain with the predicted elastic strains from dislocation model. The comparison highlights significant disagreement between the observed and the calculated strains, most clearly in the far field where the static elastic strain becomes very small. We then use these data to quantitatively examine coseismic change of pore pressure as a causal mechanism for coseismic volumetric strain, which is a mechanism not accounted for in the dislocation model. The result allows us to show that coseismic pore pressure change may play an important role to account for coseismic volumetric change both in the far and near fields and to explain the discrepancy between the observed and the calculated strains in the far field. In the near field where the coseismic elastic deformation can be appreciable, one needs to consider both the elastic volumetric strain due to faulting and the strain due to pore-pressure change in the interpretation of observed coseismic volumetric strain in the shallow crust.

2. Observation

Two basic types of observational data are available for studying coseismic changes of volumetric strain in the shallow crust. One is measured volumetric strain using various instruments; the other is volumetric strain converted from coseismic change of groundwater level in wells.

2.1. Coseismic volumetric strain from strain measurements

High quality measurements of crustal strains are usually made in boreholes, deep mines, tunnels, and other locations isolated from sources of noise at the Earth's surface. Borehole strainmeters are widely implemented because of their small size and relative economy. Detailed description of the Sacks–Evertson type dilatometer and other strainmeter designs may be found in Sacks et al. (1971) and Agnew (1986). Briefly, the dilatometer consists of a steel cylindrical container filled with fluid, which is firmly cemented to the base and the wall of a borehole. Volumetric deformation of wall rock drives fluid in the container to flow into (or out of) a freestanding flexible bellow attached to the container; deformation of the bellow is measured and calibrated to provide volumetric strain. Calibration is often made with the aid of theoretical Earth tides after the gauge is installed in the borehole. Resolution is reported to be better than 10^{-9}.

Volumetric strain may also be obtained from measurements with borehole tensor strainmeters. Detailed description of the borehole tensor strainmeters may be found in Gladwin (1984). Briefly, they consist of an array of linear strainmeters stacked vertically inside a cylindrical steel housing that in turn is cemented firmly to the wall rock of a borehole. Early strainmeter designs consisted of three horizontal linear gauges in different directions (Gladwin, 1984) that allow the determination of linear strain along an arbitrary direction in the horizontal plane, from which one can determine the areal and shear strains in this plane. Later designs include a fourth gauge to serve as a redundant check for self-consistency among gauges (Roeloffs, 2010; Qiu et al., 2013). Calibration of the gauges after installation in the borehole can be made with nearby laser strainmeters, but the latter facility is often unavailable. Thus most calibration is made with the aid of theoretical Earth tides (Roeloffs, 2010; Hodgkinson et al., 2013). The resolution of individual gauges is 10^{-10} to 5×10^{-11} (Hodgkinson et al., 2013).

Johnston et al. (2006) reported continuous measurements of borehole strain using both types of strainmeter and pore pressure in the near field of the 2004 M6.0 Parkfield earthquake in California, and showed that the measured coseismic volumetric strains are in general agreement with the prediction from the dislocation model both in the signs of the change and in the order-of-magnitude change of amplitude. These results, together with published measurements from other studies, are shown in Fig. 1(a) and listed in Table 1. The horizontal bars in the figure show the ranges of calculated coseismic strain. The large horizontal bars in some of the data clearly indicate the sensitivity of the calculated coseismic strain in the near field on the substantial uncertainties in source parameters of the dislocation model (e.g., Langbein, 2015). In the far field, the uncertainties in source parameters become less important on the calculated coseismic strain.

Qiu and Shi (2004) documented the coseismic strains from dilatometers at 17 stations in eastern China in response to the 2001 M8 Kunlun earthquake near the northern border of Tibet at a distance >2000 km from the stations (Table 1). These results together with the calculated volumetric strains from the half-space dislocation model are shown in Fig. 1(a) and included in Table 1. Most of the recorded strains are greater than 10^{-9} and some were as high as 10^{-8} with the greatest reaching 10^{-7}. The calculated coseismic strains at these stations, however, are generally of the order of 10^{-10}. In addition, about half of the recordings have opposite signs from what was predicted from the dislocation model. Zhang et al. (2017) documented volumetric strains with dilatometers in the far field of several great earthquakes (Table 1). They show that the observed co-seismic changes of static volumetric strain are greater by two to three orders of magnitude than the predicted amplitude from the dislocation model. Moreover, some observed and predicted changes have different signs.

Conversion of the coseismic areal strain measured with tensor strainmeters to the coseismic volumetric strain often makes the assumption that the coseismic change in the vertical stress is zero. Roeloffs (2010), however, suggests that the strainmeters are coupled to both areal and vertical strains, even though the coupling coefficients are uncertain. Here we assume that the vertical strain (ε_z) is related to the areal strain (ε_a) by $\varepsilon_z = -\nu\varepsilon_a/(1-\nu)$, where ν is the Poisson's ratio, and the volumetric strain (ε) is estimated from the areal strain by the relation

$$\varepsilon = \frac{(1-2\nu)}{(1-\nu)}\varepsilon_a \tag{1}$$

Furthermore, because borehole strainmeters are installed at relatively shallow depths where rocks are saturated with groundwater and because the coseismic response is nearly instantaneous, one needs to use the undrained Poisson's ratio of the wall rock in the above conversion, which can be significantly larger than the corresponding drained Poisson's ratio (Wang, 2000).

Qiu and Shi (2003) reported linear strains at Changping station near Beijing in response to two moderate earthquakes near Zhangbei in northern China; one is the Jan. 10, 1998, M6.3 earthquake and the other is the March 11, 1999, M5.8 earthquake; both at a distance of ~175 km from the station. Fu et al. (2011) reported coseismic strain from tensor strainmeters at three stations in the northern part of the Tibetan plateau in response to the 2008 M7.9 Wenchuan earthquake. The coseismic areal strain responding to several distant earthquakes are listed in Table 2; the corresponding coseismic volumetric strains, converted from the coseismic areal strains with Eq. (1) and undrained Poisson's ratio of 0.33 (Wang, 2000), are plotted in Fig. 1(a). Most of the coseismic volumetric

Table 1
Coseismic volumetric strain (in microstrain, dilatation positive) documented by dilatometers compared with predicted elastic strain from dislocation model for several earthquakes.

Site	Earthquake	M	Distance (km)[a]	Observed vol. strain	Calculated vol. strain	Reference
GH	1994 Parkfield, CA	4.7	16.9	−0.016	−0.004	Quilty and Roeloffs (1997)
FR	1994 Parkfield, CA	4.7	9.2	−0.026	−0.020	Quilty and Roeloffs (1997)
DL	1994 Parkfield, CA	4.7	10.0	+0.086	+0.090	Quilty and Roeloffs (1997)
FRD[b]	2004 Parkfield, CA	6.0	15.0	−0.610	−0.100, −2.200	Johnston et al. (2006)
DLD[b]	2004 Parkfield, CA	6.0	16.6	+0.840	+0.130, +1.800	Johnston et al. (2006)
JCD[b]	2004 Parkfield, CA	6.0	20.4	−0.284	−0.110, −0.070	Johnston et al. (2006)
RHD[b]	2004 Parkfield, CA	6.0	25.0	+0.058	+0.200, +0.160	Johnston et al. (2006)
VCD[b]	2004 Parkfield, CA	6.0	20.4	−4.776	−0.200, +0.120	Johnston et al. (2006)
CHCH[c]	2008 Kunlun, China	8.1	3250	+0.002	−0.0004	Qiu and Shi (2004)
FX[c]	2008 Kunlun, China	8.1	2870	+0.053	−0.0005	Qiu and Shi (2004)
JZH[c]	2008 Kunlun, China	8.1	2810	+0.003	−0.0005	Qiu and Shi (2004)
ZHJK[c]	2008 Kunlun, China	8.1	2250	+0.003	−0.0011	Qiu and Shi (2004)
HL[c]	2008 Kunlun, China	8.1	2300	−0.012	−0.0009	Qiu and Shi (2004)
CHP[c]	2008 Kunlun, China	8.1	2360	+0.023	−0.0008	Qiu and Shi (2004)
YT[c]	2008 Kunlun, China	8.1	2780	0.0	−0.0001	Qiu and Shi (2004)
AQ[c]	2008 Kunlun, China	8.1	2580	+0.001	0.00	Qiu and Shi (2004)
XY[c]	2008 Kunlun, China	8.1	2090	−0.004	−0.0004	Qiu and Shi (2004)
CHQ[c]	2008 Kunlun, China	8.1	2330	−0.280	0.00	Qiu and Shi (2004)
TA[c]	2008 Kunlun, China	8.1	2390	+0.001	0.00	Qiu and Shi (2004)
XZH[c]	2008 Kunlun, China	8.1	2400	+0.002	+0.0004	Qiu and Shi (2004)
NJ[c]	2008 Kunlun, China	8.1	2590	−0.002	+0.0005	Qiu and Shi (2004)
LY[c]	2008 Kunlun, China	8.1	2650	−0.003	+0.0005	Qiu and Shi (2004)
NT[c]	2008 Kunlun, China	8.1	2790	−0.003	+0.0005	Qiu and Shi (2004)
QZH[c]	2008 Kunlun, China	8.1	2810	0.0	+0.0008	Qiu and Shi (2004)
SHZH[c]	2008 Kunlun, China	8.1	2610	+0.001	+0.0011	Qiu and Shi (2004)
Fuxin[c]	2008 Wenchuan, China	7.9	1439	+0.331	+0.0003	Zhang et al. (2017)
Fuxin[c]	2011 Tohoku, Japan	9.1	1236	+0.488	+0.010	Zhang et al. (2017)
Fuxin[c]	2012 Sumatra	8.6	5423	+0.113	−0.0001	Zhang et al. (2017)

[a] Hypocenter distance.
[b] Central California.
[c] Eastern China.

strains reported by Fu et al. (2011) are one to two orders of magnitude greater than the calculated strains from the dislocation model (Fig. 1(a) and Table 2).

Barbour et al. (2015) used a probabilistic detection method to estimate coseismic offsets produced by 34 earthquakes on nine borehole strainmeters operated by the Plate Boundary Observatory (PBO) in southern California. The coseismic volumetric strains are converted from the offsets in instrumental strains and are plotted against the calculated strain for a dislocation model in Fig. 1. In general, most observed volumetric strains differ substantially in their absolute magnitudes from the static strain predicted by elastic dislocation theory and some are of opposite signs.

In summary, a large number of existing borehole strain measurements, especially those in the far field of earthquakes, show absolute magnitudes of the measured coseismic volumetric strain far exceeding that predicted by elastic dislocation theory.

2.2. Coseismic volumetric strain estimated from water-level change in wells

Because coseismic volumetric strain and pore pressure in aquifers are causally related, measurement of coseismic change in water level in wells provides an indirect observation of coseismic volumetric strain (e.g., Quilty and Roeloffs, 1997). Three distinct mechanisms can cause coseismic water-level changes – coseismic consolidation (e.g., Wang et al., 2001), undrained loading (Skempton, 1960) and coseismic recharge from a source or discharge to a sink (e.g., Roeloffs, 1998; Wang et al., 2017). The mechanism of coseismic consolidation applies only to unconsolidated sediments. Because strain gauges are commonly mounted on crystalline rocks or consolidated sedimentary rocks, we only consider the latter two mechanisms that are relevant for the coseismic elastic strain.

For water-level change due to undrained loading that may be significant for aquifers relatively close to the earthquake source, the amplitude of the coseismic pore pressure change in the aquifer, Δp (in Pa), is linked to the amplitude of the coseismic undrained volumetric strain change, $\Delta\varepsilon$, by the Skempton relation; i.e.,

$$\Delta p = -B\Delta\sigma = -BK_u\Delta\varepsilon_u \tag{2}$$

where B is the dimensionless Skempton coefficient, $\Delta\sigma$ the change of mean stress in Pa, K_u the undrained bulk modulus in Pa and $\Delta\varepsilon_u$ the change of volumetric strain in undrained loading. The usual procedure for estimating the product BK_u is by taking the ratio between the amplitude of measured tidal oscillations of water level in wells and the amplitude of the theoretical strain. The tidal amplitude of pore pressure is related to that of water level in wells, Δh (in m), by the relation

$$\Delta p = \rho g \Delta h \tag{3}$$

where ρ is water density in kg/m^3 and g the gravitational acceleration in m s^{-2}. Assuming the same efficiency for the earthquake-induced water-level change, we may convert the co-seismic change of water level during earthquakes due to undrained loading to coseismic change in volumetric strain by the following relation,

$$\Delta\varepsilon_u = -\rho g \Delta h/(BK_u). \tag{4}$$

Direct comparison between the volumetric strain estimated from coseismic change of water level and the calculated coseismic strain is relatively few because it requires both measurement of pore pressure and analysis of tidal response of water level in the same well for the evaluation of BK_u of the wall rock. Such

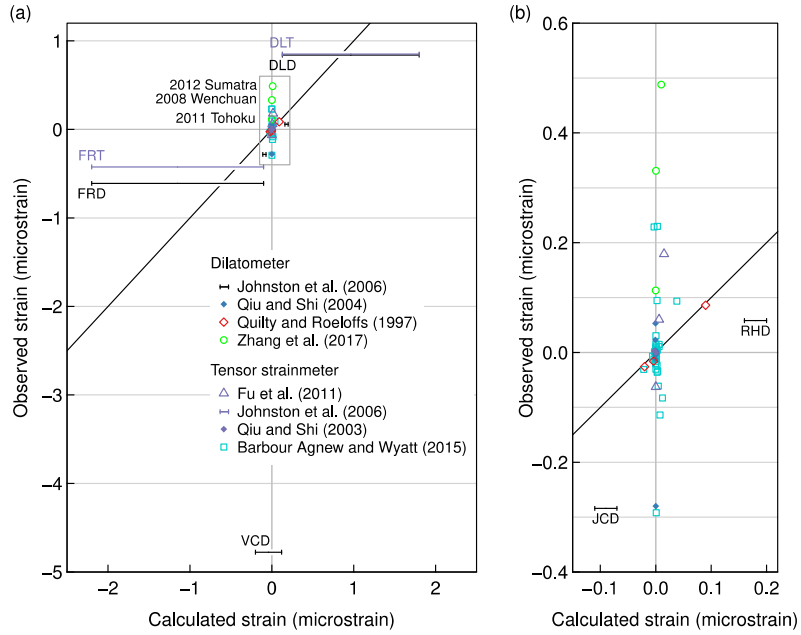

Fig. 1. (a) Observed coseismic volumetric strain from dilatometer measurement, plotted against predicted coseismic volumetric strain from dislocation model. Data enclosed in the small rectangle is enlarged in (b). (b) Enlarged view of the group of data enclosed in the small rectangle in (a) showing that most observed volumetric strains in the intermediate and far fields of earthquakes have absolute magnitude far exceeding the volumetric strain predicted from dislocation model.

Table 2
Coseismic areal strains (in microstrain, dilatation positive) documented by tensor strainmeters compared with predicted elastic strain from dislocation model for several earthquakes.

Site	Earthquake	M	Distance (km)[b]	Observed areal strain[c]	Calculated areal strain[d]	Reference
B084	2010 El Mayor-Cucapah earthquake	7.2	186	−0.170	0.057	Barbour et al. (2015)
FRT	2004 Parkfield	6.0	15.0	−0.425	−0.1, −2.2	Johnston et al. (2006)
DLT	2004 Parkfield	6.0	16.6	+0.850	+0.13, +1.8	Johnston et al. (2006)
Changping [a]	1998 Zhangbei 1	6.3	175	+0.0031	−0.0026	Qiu and Shi (2003)
Changping[a]	1999 Zhangbei 2	5.8	175	−0.0003	−0.00005	Qiu and Shi (2003)
Guza[a]	2008 Wenchuan	7.9	140	−0.0626	∼0	Fu et al. (2011)
Yushu[a]	2008 Wenchuan	7.9	700	+0.1795	+0.015	Fu et al. (2011)
Golmud[a]	2008 Wenchuan	7.9	1000	+0.0601	+0.006	Fu et al. (2011)

[a] Chinese stations.
[b] Hypocenter distance.
[c] Converted from areal strain using Eq. (1), assuming $\nu = 0.33$.
[d] Calculated from half-space model.

requirements are not fulfilled at most wells. In some situations BK_u can be estimated directly: at some stations of the PBO borehole network, pore pressure measurements are collocated with the strainmeters, allowing for comprehensive characterization of the quasistatic response to tides, atmospheric pressure changes, and teleseismic waves (Barbour, 2015).

Quilty and Roeloffs (1997) made a comprehensive analysis of water-level responses of nine wells near Parkfield, CA, that responded to a small (M4.7) local earthquake. The authors demonstrated that three of the borehole dilatometers and four of the wells showed coseismic water-level changes in good agreement with that predicted by a dislocation model. At the other sites, however, the agreement is poor and some are of opposite signs (Fig. 2; Table 3). Grecksch et al. (1999) analyzed water-level records of 194 continuously operating well-level gauges in Germany responding to a moderate earthquake (M5.4); they found that the observed amplitudes of the coseismic steps are much greater than those calculated from a dislocation model. Zhang et al. (2017) documented the response of water level in a well in China in response to several large earthquakes in the intermediate and far fields; they showed that the strains inferred from water-level changes at the well exceed those predicted by the dislocation model by two to three orders of magnitude (Fig. 2; Table 3). Furthermore, Koizumi et al. (2004) calculated the static volumetric strain changes due to the 1999 M7.6 Chi-Chi earthquake, Taiwan, using the dislocation model. The signs of the calculated changes were largely opposite in sign to that of the observed water level changes (Wang et al., 2001; Chia et al., 2001). Finally, Yan et al. (2014) showed that the calculated coseismic static volumetric strains due to the 2010 M9.2 Tohoku earthquake using a dislocation model are largely of opposite signs from that of the observed coseismic strains converted from water level changes.

3. Discussion

As noted in Introduction several hypotheses have been proposed to explain the discrepancies between the observed coseismic volumetric strain and the strain predicted from the theoretical dislocation model. But none has been quantitatively tested. Motivated by the widely documented coseismic water-level changes in wells at great epicentral distances where both the static strain and ground-motion are negligible (e.g., Wang and Manga, 2010; Weingarten and Ge, 2014; Manga and Wang, 2015), we use the data discussed in the last section to quantitatively test the hypothesis that coseismic change of pore pressure in the shallow crust

Table 3
Coseismic volumetric strains (in microstrain, dilatation positive) converted from coseismic water-level change compared with the predicted strains from dislocation model for several earthquakes.

Well	Earthquake	M	Distance (km)[a]	Vol. strain from water level[c]	Predicted vol. strain[d]	Reference
B084	2010 El Mayor-Cucapah earthquake	7.2	186	−0.61	+0.028	This study
FF	1994 Parkfield, CA	4.7	∼10[e]	+0.110	+0.140	Quilty and Roeloffs (1997)
VW	1994 Parkfield, CA	4.7	∼9[e]	+0.017	+0.026	Quilty and Roeloffs (1997)
JC	1994 Parkfield, CA	4.7	∼10[e]	+0.160	+0.140	Quilty and Roeloffs (1997)
TF	1994 Parkfield, CA	4.7	12.5	+0.190	+0.040	Quilty and Roeloffs (1997)
CS	1994 Parkfield, CA	4.7	∼17[e]	0.00	+0.001	Quilty and Roeloffs (1997)
GH	1994 Parkfield, CA	4.7	16.9	−0.035	−0.003	Quilty and Roeloffs (1997)
MM	1994 Parkfield, CA	4.7	∼10[e]	+0.200	−0.060	Quilty and Roeloffs (1997)
MS	1994 Parkfield, CA	4.7	∼10[e]	+0.210	−0.070	Quilty and Roeloffs (1997)
HR	1994 Parkfield, CA	4.7	∼11[e]	+0.870	+0.090	Quilty and Roeloffs (1997)
Fuxin[b]	2008 Wenchuan, China	7.9	1439	+0.417	+0.0003	Zhang et al. (2017)
Fuxin[b]	2011 Tohoku, Japan	9.1	1236	+1.396	+0.010	Zhang et al. (2017)
Fuxin[b]	2012 Sumatra	8.6	5423	+0.384	−0.0001	Zhang et al. (2017)

[a] Hypocenter distance.
[b] Station in eastern China.
[c] Converted using Eq. (4) and BK_u values estimated from tidal analysis.
[d] Calculated from half-space elastic strain model.
[e] Epicenter distance estimated from Fig. 1 in Quilty and Roeloffs (1997).

may explain the discrepancy between observed and calculated coseismic volumetric strains.

3.1. Poroelastic coupling mechanisms

We first illustrate the distinct poroelastic coupling mechanisms at work in determining the coseismic responses of pore pressure and volumetric strain. In Fig. 3(a) we display the records from a Plate Boundary Observatory borehole (B084) in southern California in response to the 2010 Mw7.2 El Mayor-Cucapah earthquake. Before the earthquake, pore pressure and volumetric strain responded to solid tides with the expected oscillations of opposite signs. During the earthquake, volumetric strain suddenly decreased while pore pressure immediately increased. After the earthquake, pore pressure continued to rise to a peak and then declined gradually towards the pre-seismic level. Here the coseismic increase of pore pressure is opposite in direction to the change in volume, similar to their response to solid tides; thus the coseismic increase of pore pressure was caused by coseismic volumetric contraction.

We next display in Fig. 3(b) the records from Fuxin well in northeastern China in response to the 2011 Mw9.1 Tohoku earthquake (Zhang et al., 2017). Here the increase of water level (pore pressure) is associated with an *increase* in volumetric strain, suggesting that the latter was caused by the increase of pore pressure. Earlier studies (e.g., Roeloffs, 1998; Wang et al., 2017) showed that both increase or decrease of water level may occur and may be explained by recharge from a source (or discharge to a sink) near the well. Two types of source/sink may occur, depending on local geologic settings: One is groundwater in terrains with different elevations, which connects to wells due to earthquake-enhanced permeability (Rojstaczer et al., 1995; Roeloffs, 1998; Wang et al., 2004; Wang and Manga, 2015); the other is heterogeneous source/sink in shallow crust (Roeloffs, 1998; Wang et al., 2017), which connects to wells by enhanced permeability. In such cases, groundwater flow occurs and it is incorrect to convert water-level change to volumetric strain using Skempton's relation (2) that is specifically for pore-pressure response under undrained loading.

To further illustrate the relation between the coseismic volumetric strain and pore pressure, we plot in Fig. 4 the coseismic volumetric strain measured with strainmeters against the volumetric strain converted from collocated water-level measurement. Only five pairs of such data have been found (Table 4) partly because collocated measurements of both coseismic volumetric strain and water level are rare, and partly because the conversion of coseismic change of water level to volumetric strain needs calibration by tidal responses that are absent in many wells.

The line with a slope of 1 in Fig. 4 represents the case when coseismic volumetric strain from strain-gauge measurement is equal to coseismic volumetric strain converted from water level change. Two of the five data points at moderate epicenter distances (Table 4) fall close to the linear relation; the other data points with great epicenter distances, however, deviate largely from the relation. For the latter data points, volumetric strain change was converted from the amplitude of water-level change using Skempton relation (Zhang et al., 2017); this procedure, as pointed out above, is incorrect for processes involving groundwater flow. The correct equation to use in such cases is instead Biot's relation (Biot, 1941) that relates the change of volumetric strain of saturated poroelastic media to changes of both the mean normal stress and pore pressure. For isotropic poroelastic media, Biot's relation is

$$\Delta\varepsilon_d = \frac{1}{K}(\Delta\sigma + \alpha\Delta p) \tag{5}$$

where $\Delta\varepsilon_d$ is the change of volumetric strain in a drained condition, K the drained bulk modulus of the porous medium in Pa, $\Delta\sigma$ the change of the mean normal stress in Pa, α the dimensionless Biot–Willis coefficient and Δp the change of pore pressure in Pa. Since the well in Zhang et al. (2017) was far from the earthquakes (Table 1), $\Delta\sigma$ is negligible; thus

$$\Delta\varepsilon_d = \frac{\alpha}{K}(\Delta p) \tag{6}$$

Comparing this relation with Eq. (4) and noting $K/K_u = (1 - \alpha B)$ and $\alpha B = 3(\nu_u - \nu)/[(1 - 2\nu)(1 + \nu_u)]$ (Wang, 2000), we obtain a correction to the undrained volumetric strain calculated in (Zhang et al., 2017) as

$$\Delta\varepsilon_d = \alpha B\frac{K_u}{K}|\Delta\varepsilon_u| = \frac{3(\nu_u - \nu)}{(1 + \nu)(1 - 2\nu_u)}|\Delta\varepsilon_u| \tag{7}$$

Assuming $\nu = 0.25$ and $\nu_u = 0.33$ (Wang, 2000) we have $\Delta\varepsilon_d = 0.58|\Delta\varepsilon_u|$. The corrected volumetric strain, shown in open squares in Fig. 4, fall much closer to the line with a slope of 1, further supporting the hypothesis that the change of volumetric strain was caused by pore pressure change due to external recharge.

Thus the above model suggests that coseismic volumetric strain in shallow crust is basically a combination of the elastic strain from fault rupture and the strain produced by pore pressure. It is important to recognize that these different mechanisms lead to different

Table 4
Measured coseismic volumetric strains (in microstrain, dilatation positive) for several earthquakes compared with coseismic strains converted from water-level change. (Data for strains measured with strainmeters are taken from Tables 1 and 2; Data for strains converted from water-level changes are taken from Table 3.)

Well	Earthquake	M	Measured vol. strain with strainmeter	Converted vol. strain from water level	Corrected vol. strain from water-level strain (this study, see text)
B084	2010 El Mayor-Cucapah earthquake	7.2	−0.085 (this study)	−0.061 (this study)	–
GH	1994 Parkfield, CA	4.7	−0.016[a]	−0.035[b]	–
Fuxin[b]	2008 Wenchuan, China	7.9	+0.331[a]	+0.417[b]	+0.192
Fuxin[b]	2011 Tohoku, Japan	9.1	+0.488[a]	+1.396[b]	+0.810
Fuxin[b]	2012 Sumatra	8.6	+0.113[a]	+0.384[b]	+0.213

[a] From Table 1.
[b] From Table 3.

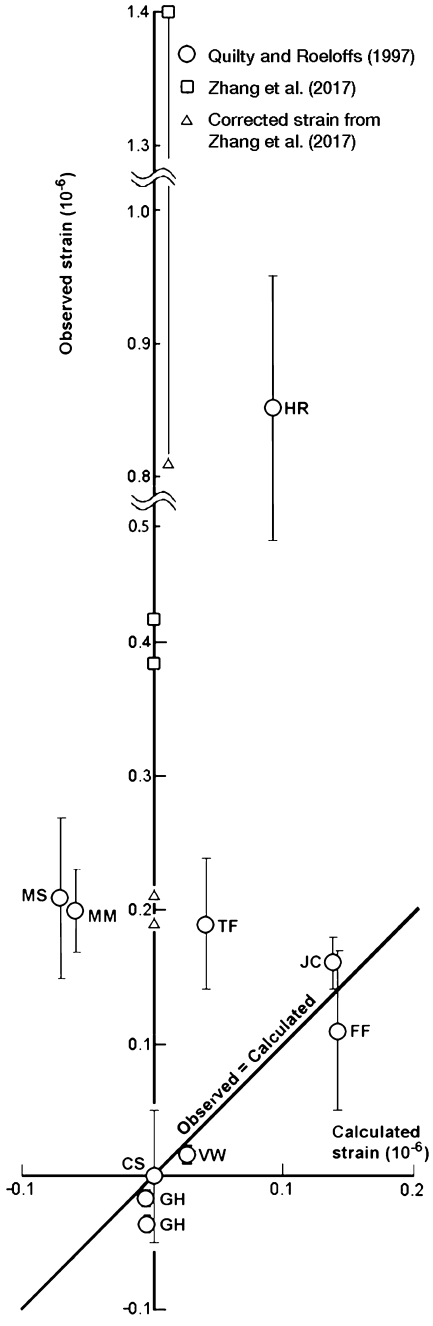

Fig. 2. Observed coseismic volumetric strain converted from data for coseismic change of water level, plotted against predicted coseismic volumetric strain from dislocation model. Correction of strains from Zhang et al. (2017) is discussed in text (see also Table 4).

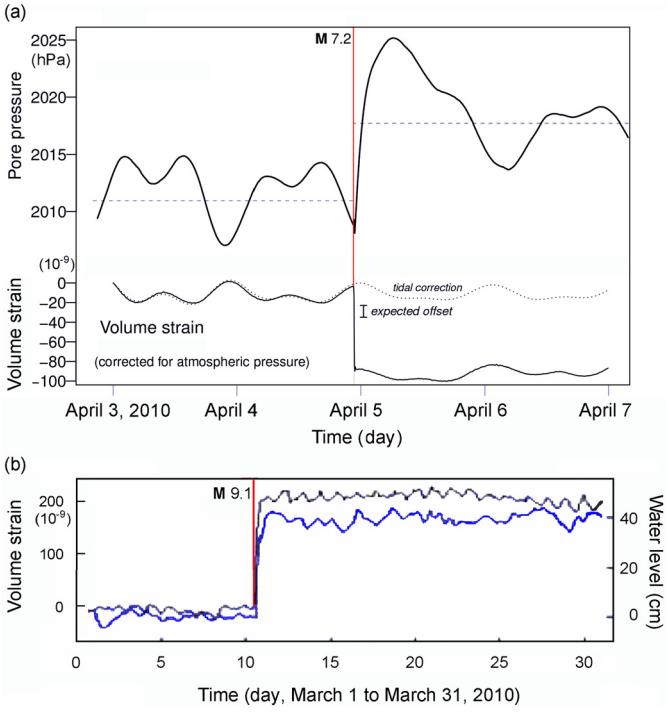

Fig. 3. (a) Pore pressure and volumetric strain in PBO borehole B084 in southern California, before and after the 2010 Mw7.2 El Mayor-Cucapah earthquake in Mexico. Negative strain shows contraction. A coseismic change of pore pressure of 670 Pa is estimated by fitting a set of sinusoids (for the tides), a trend, and a step function at the time of the earthquake to pore pressure data. (b) Water level (lower curve) and volumetric strain (upper curve) in Fuxin well in northeastern China, before and after the 2011 Mw9.1 Tohoku earthquake, Japan (modified from Zhang et al., 2017).

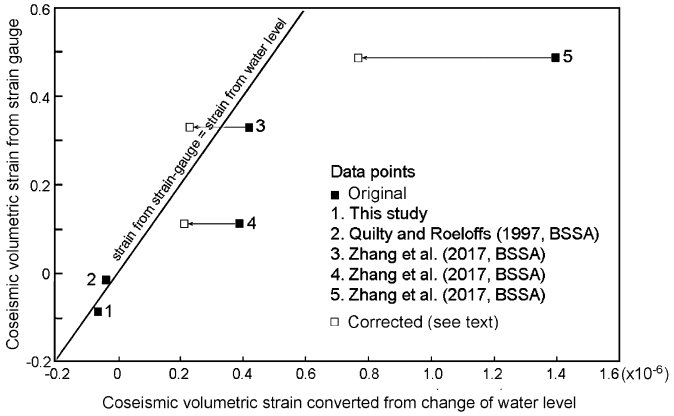

Fig. 4. Coseismic volumetric strain measured with strainmeters plotted against coseismic volumetric strain from coseismic change of water level in wells.

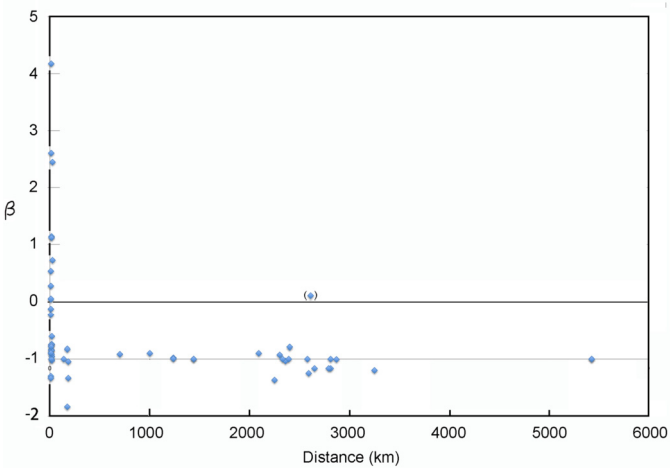

Fig. 5. Plot of the discrepancy index, β, as defined in Eq. (8) against epicentral distance for all wells in this study.

poroelastic coupling, i.e., solid to fluid vs. fluid to solid, resulting in strain and pressure changes that are either 180° out of phase or in phase. Thus in the near field, the static volumetric strain may be so large (in absolute value) that it becomes the dominant factor in affecting the change of pore pressure; here the change of pore pressure will show opposite sign from that of the volumetric strain (Fig. 3(a)). In the far field, the change of static volumetric strain may be negligibly small, while dynamic strain associated with surface waves may be sufficiently large to change rock permeability (e.g., Brodsky et al., 2003; Manga et al., 2012) that may lead to coseismic recharge (e.g., Wang et al., 2017) to change pore pressure and thus volumetric strain. In this case, the change of pore pressure will show the same sign as that of the change of volumetric strain (Fig. 3(b)).

3.2. Model testing

Finally we subject the model to a quantitative test. The model predicts that coseismic volumetric strain in the far field may be dominated by, and thus have the same sign as, the change of pore pressure. In the near field, on the other hand, coseismic volumetric strain may either have the same sign as, or of opposite sign from, that predicted by the dislocation model, depending on the relative effects of the elastic strain and the pore-pressure strain. If the two contributions have the same sign, the observed strain will be greater than the calculated strain; on the other hand, if the two contributions have opposite signs they may cancel each other and thus the observed strain will be smaller than the calculated strain and may even have opposite sign. For testing these predictions we define a 'discrepancy index' as

$$\beta = \big[(\text{coseismic elastic volumetric strain from dislocation model})/ (\text{coseismic observed volumetric strain})\big] - 1. \quad (8)$$

The discrepancy index β would be zero if the observed volumetric strain is consistent with the elastic dislocation model. We plot in Fig. 5 β against epicenter distance for all the wells in this study (Tables 1, 2 and 3); it shows that, except a few exceptions, most wells show β values significantly different from zero.

To interpret this plot we recall the basic assumption of the model that the observed coseismic strain is the sum of the coseismic elastic strain due to fault rupture and the strain due to coseismic pore-pressure change. Thus we may rewrite Eq. (8) as

$$\beta = -\big[(\text{coseismic pore-pressure produced strain})/ \big((\text{coseismic elastic strain from dislocation model}) + (\text{coseismic pore-pressure produced strain})\big)\big] \quad (9)$$

The model predicts that $\beta = 0$ if pore pressure is insignificant in affecting the observed volumetric strain, $\beta \sim -1$ if pore pressure has a dominant effect on the observed strain, and β may either be positive or negative if both the pore pressure strain and the elastic dislocation strain are significant, and its absolute magnitude may either be smaller than 1 if the fault rupture effect and the pore-pressure effect have the same sign or greater than 1 if the two effects have opposite signs. Fig. 5 shows that at epicenter distances greater than 100 km all data points (except one in parenthesis) show β close to -1, i.e., that pore pressure has a dominant effect on the observed strain. At distances <100 km, β shows large scatter with both positive and negative with absolute value either greater or less than 1. Thus pore pressure may have a significant effect on the observed strain even in the near field. We may thus conclude that pore pressure may play an important role in producing coseismic volumetric strain both in the near field and in the far field of earthquakes.

As an addendum to the model we note that, since linear strains in arbitrary direction may be decomposed into normal and shear strains and the normal strain is affected by pore pressure, interpretation of observed coseismic linear strains and the associated crust deformation needs to account for both the strain due to fault rupture and that produced by pore pressure change.

Acknowledgement

The senior author thanks Douglas Dreger, Michael Manga, Yan Zhang, Lian Xue and Adrian Borsa for discussion. The authors thank Evelyn Roeloffs, Ruth Harris, Elco Luijendijk and an anonymous reviewer for their constructive reviews. Work was supported by NSF grant EAR1344424 to C.Y.W.

References

Agnew, D.C., 1986. Strainmeters and tiltmeters. Rev. Geophys. 24 (3), 579–624. http://dx.doi.org/10.1029/RG024i003p00579.

Barbour, A.J., 2015. Pore pressure sensitivities to dynamic strains: observations in active tectonic regions. J. Geophys. Res., Solid Earth 120, 5863–5883. http://dx.doi.org/10.1002/2015JB012201.

Barbour, A.J., Agnew, D.C., Wyatt, F.K., 2015. Coseismic strains on plate boundary observatory borehole strainmeters in Southern California. Bull. Seismol. Soc. Am. 105, 431–444.

Beaumont, C., Berger, J., 1975. An analysis of tidal strain observations from the United States of America: 1. The laterally homogeneous tide. Bull. Seismol. Soc. Am. 65, 1613–1629.

Biot, M.A., 1941. General theory of three-dimensional consolidation. J. Appl. Phys. 12, 155–164.

Bletery, Q., Thomas, A.M., Rempel, A.W., Karlstrom, L., Sladen, A., De Barros, L., 2016. Mega-earthquakes rupture flat megathrusts. Science 354, 1027–1031.

Brodsky, E.E., Roeloffs, E., Woodcock, D., Gall, I., Manga, M., 2003. A mechanism for sustained ground water pressure changes induced by distant earthquakes. J. Geophys. Res. 108. http://dx.doi.org/10.1029/2002JB002321.

Burgmann, R., Segall, P., Lisowski, S., Svarc, J., 1997. Postseismic strain following the 1989 Loma Prieta earthquake from GPS and leveling measurements. J. Geophys. Res. 102, 4933–4955.

Chia, Y.P., Wang, Y.S., Wu, H.P., Chiu, J.J., Liu, C.W., 2001. Changes of groundwater level due to the 1999 Chi-Chi earthquake in the Choshui River fan in Taiwan. Bull. Seismol. Soc. Am. 91, 1062–1068.

Fu, G., Shen, X., Yoichi, F., Gao, S., Yoshii, S., 2011. Co-seismic strain changes of Wenchuan Mw7.9 earthquake recorded by borehole strainmeters on Tibetan plateau. Geod. Geodyn. 2, 42–49.

Gladwin, M.T., 1984. High precision multi-component borehole deformation monitoring. Rev. Sci. Instrum. 55, 2011–2016.

Grecksch, G., Roth, F., Kümpel, H.-J., 1999. Coseismic well-level changes due to the 1992 Roermond earthquake compared to static deformation of half-space solutions. Geophys. J. Int. 138, 470–478.

Harris, R.A., Simpson, R.W., 1992. Changes in static stress on southern California faults after the 1992 Landers earthquake. Nature 360, 251–254.

Hodgkinson, K., Langbein, J., Henderson, B., Mencin, D., Borsa, A., 2013. Tidal calibration of plate boundary observatory borehole strainmeters. J. Geophys. Res., Solid Earth 118, 447–458. http://dx.doi.org/10.1029/2012JB009651.

Hughes, K.L.H., Masterlark, T., Mooney, W.D., 2010. Poroelastic stress-triggering of the 2005 M8.7 Nias earthquake by the 2004 M9.2 Sumatra–Andaman earthquake. Earth Planet. Sci. Lett. 293, 289–299. http://dx.doi.org/10.1016/j.epsl.2010.02.043.

Johnston, M.J.S., Borcherdt, R.D., Linde, A.T., Gladwin, M.T., 2006. Continuous borehole strain and pore pressure in the near field of the 2004 M6.0 Parkfield, California, earthquake: implications for nucleation, fault response, earthquake prediction, and tremor. Bull. Seismol. Soc. Am. 96, S56–S72. http://dx.doi.org/10.1785/0120050822.

King, G.C.P., Stein, R.S., Lin, J., 1994. Static stress changes and the triggering of earthquakes. Bull. Seismol. Soc. Am. 84, 935–953.

Koizumi, N., Lai, W.-C., Kitagawa, Y., Matsumoto, Y., 2004. Comment on "Coseismic hydrological changes associated with dislocation of the September 21, 1999 Chichi earthquake, Taiwan" by Min Lee et al.. Geophys. Res. Lett. 31, L13603. http://dx.doi.org/10.1029/2004GL019897.

Kroll, K.A., Cochran, E.S., Murray, K.E., 2017. Poroelastic properties of the Arbuckle Group in Oklahoma derive from well fluid level response to the 3 September 2016 Mw5.8 Pawnee and 7 November 2016 Mw5.0 Cushing earthquakes. Seismol. Res. Lett. 88, 963–970. http://dx.doi.org/10.1785/0220160228.

Langbein, J., 2015. Borehole strainmeter measurements spanning the 2014 Mw6.0 South Napa Earthquake, California: the effect from instrument calibration. J. Geophys. Res., Solid Earth 120, 7190–7202. http://dx.doi.org/10.1002/2015JB012278.

Manga, M., Beresnev, I., Brodsky, E.E., et al., 2012. Changes in permeability by transient stresses: field observations, experiments and mechanisms. Rev. Geophys. 50, RG2004. http://dx.doi.org/10.1029/2011RG000382.

Manga, M., Wang, C.-Y., 2015. Earthquake hydrology. In: Treatise on Geophysics, vol. 4, 2nd edition, pp. 305–328.

Okada, Y., 1985. Surface deformation due to shear and tensile faults in a half-space. Bull. Seismol. Soc. Am. 75, 1135–1154.

Press, F., 1965. Displacement, strains, and tilts at teleseismic distances. J. Geophys. Res. 70, 2395–2412.

Qiu, Z., Shi, Y., 2003. Observations of remote coseismic stress step-changes. Sci. China, Ser. D 46 (Suppl.), 75–81.

Qiu, Z., Shi, Y., 2004. Application of observed strain steps to the study of remote earthquake stress triggering. Acta Seismol. Sin. 17, 534. http://dx.doi.org/10.1007/s11589-004-0035-z.

Qiu, Z., Tang, L., Zhang, B., Guo, Y., 2013. In situ calibration of and algorithm for strain monitoring using four-gauge borehole strainmeters (FGBS). J. Geophys. Res., Solid Earth 118, 1609–1618. http://dx.doi.org/10.1002/jgrb.50112.

Quilty, E.G., Roeloffs, E.A., 1997. Water-level changes in response to the 20 December 1994 Earthquake near Parkfield, California. Bull. Seismol. Soc. Am. 87, 310–317.

Roeloffs, E., 1998. Persistent water level changes in a well near Parkfield, California, due to local and distant earthquakes. J. Geophys. Res. 103, 869–889.

Roeloffs, E., 2010. Tidal calibration of Plate Boundary Observatory borehole strainmeters: roles of vertical and shear coupling. J. Geophys. Res. 115, B06405. http://dx.doi.org/10.1029/2009JB006407.

Roeloffs, E.A., Nelms, D.L., Sheets, R.A., 2015. Widespread groundwater-level offsets caused by the Mw5.8 Mineral, Virginia, earthquake of 23 August 2011. In: Horton, J.W. Jr., Chapman, M.C., Green, R.A. (Eds.), The 2011 Mineral, Virginia, Earthquake, and Its Significance for Seismic Hazards in Eastern North America. In: Spec. Pap., Geol. Soc. Am., vol. 509, pp. 117–136.

Rojstaczer, S., Wolf, S., Michel, R., 1995. Permeability enhancement in the shallow crust as a cause of earthquake-induced hydrological changes. Nature 373, 237–239.

Rybicki, K., 1973. Analysis of aftershocks on the basis of dislocation theory. Phys. Earth Planet. Inter. 7, 409–422.

Sacks, I.S., Suyehiro, S., Evertson, D.W., Yamagishi, Y., 1971. Sacks–Evertson strainmeter, its installation in Japan and some preliminary results concerning strain steps. Pap. Meteorol. Geophys. 22, 195–207.

Simpson, R.W., Reasenberg, P.A., 1994. Earthquake-induced static stress changes on central California faults, The Loma Prieta, California Earthquake of October 17, 1989 – Tectonic processes and models. In: Simpson, R.W. (Ed.), U. S. Geol. Surv. Prof. Pap., vol. 1550-F, pp. F55–F89.

Skempton, A.W., 1960. Terzaghi's discovery of effective stress. In: Bjerrum, L., Casagrande, A., Peck, R.B., Skempton, A.W. (Eds.), From Theory to Practice in Soil Mechanics. John Wiley, New York, pp. 42–53.

Stein, R.S., Lisowski, M., 1983. The 1979 Homestead valley earthquake sequence, California: control of aftershocks and postseismic deformation. J. Geophys. Res. 88, 6477–6490.

Wang, H.F., 2000. Theory of Linear Poroelasticity. Princeton Ser. Geophys. Princeton Univ. Press, Princeton, NJ.

Wang, C.-Y., Cheng, L.H., Chin, C.V., Yu, S.B., 2001. Coseismic hydrologic response of an alluvial fan to the 1999 Chi-Chi earthquake, Taiwan. Geology 29, 831–834.

Wang, C.-Y., Wang, C.H., Manga, M., 2004. Coseismic release of water from mountains: evidence from the 1999 ($M_w = 7.5$) Chi-Chi, Taiwan, earthquake. Geology 32, 769–772.

Wang, C.-Y., Manga, M., 2010. Earthquakes and Water. Lect. Notes Earth Sci., vol. 114. Springer, Berlin. 249 pp.

Wang, C.-Y., Manga, M., 2015. New streams and springs after the 2014 Mw6.0 South Napa earthquake. Nat. Commun. 6, 7597. http://dx.doi.org/10.1038/ncomms8597.

Wang, C.-Y., Manga, M., Shirzaei, M., Weingarten, M., Wang, L.-P., 2017. Induced seismicity in Oklahoma affects shallow groundwater. Seismol. Res. Lett. 88. http://dx.doi.org/10.1785/0220170017.

Weingarten, M., Ge, S., 2014. Insights into water level response to seismic waves: a 24 year high-fidelity record of global seismicity at Devils Hole. Geophys. Res. Lett. 41, 74–80. http://dx.doi.org/10.1002/2013GL058418.

Yan, R., Woith, H., Wang, R., 2014. Groundwater level changes induced by the 2011 Tohoku earthquake in China mainland. Geophys. J. Int. 199, 533–548. http://dx.doi.org/10.1093/gji/ggu196.

Zhang, Y., Wang, C.-Y., Fu, L.-Y., Yan, R., Chen, X., 2017. Mechanism of the coseismic change of volumetric strain in the far field of earthquakes. Bull. Seismol. Soc. Am. 107, 475–481.